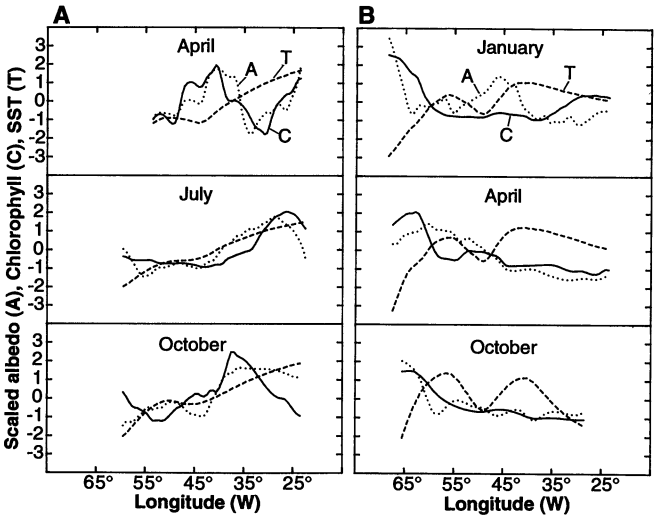

Fig. 2. Representative spatial and seasonal distributions of averaged (*8*), scaled cloud albedo (A, dotted lines), SST (T, dashed lines), and phytoplankton chlorophyll (C, solid lines). Each variable was scaled by $(x_i - x)/\sigma$, where x_i is the observed value, x is the mean, and σ is the standard deviation. Data from two latitude bands are presented, (**A**) from 57° to 60°N and (**B**) from 38° to 43°N. In these figures, the chlorophyll values were shifted 400 km downwind (*8*).

some groups of phytoplankton, such as chromophytes and coccolithophorids, more than other groups, such as diatoms or cyanobacteria (*12*). The increase in both albedo and chlorophyll between 52° and 60°W in April (Fig. 2A) corresponds to coccolithophore blooms off the coast of Iceland in the summer and to high DMS concentrations in the upper ocean (*13*). At lower latitudes, however, there are insufficient data on the temporal and spatial distributions of coccolithophores or other major DMS producers. It is possible that the relation between DMS and chlorophyll on the large spatial scales examined here may be more robust than on the small scales normally examined by surface vessels (*14*).

Analysis of the relation between SST and albedo indicated that in some regions higher albedo was associated with high SST; however, in 40% of the regions high albedo was associated with low SST. Although a multivariate model could be developed for each region with SST and chlorophyll used to predict albedo (*15*), our results suggest that the relation among the albedo of marine stratus clouds, cloud temperature, and SST is complex and cannot be generalized for the basin throughout the year.

We conclude that, near the continental margin, both natural and anthropogenic processes can contribute to the enhanced albedo of marine stratus clouds; we cannot quantitatively apportion the relative importance of these two factors from the available data. Over the central North Atlantic Ocean basin, however, much of the variability in albedo appears to be related solely to natural factors. Although over the last 100 years anthropogenic sulfate emissions have increased exponentially, natural marine emissions of DMS probably have remained relatively constant (*16*). The anthropogenic emissions appear to have affected noncloud reflectivity (*17*); however, the effect of human activities on cloud albedo appears to be minimal in the remote marine environment.

REFERENCES AND NOTES

1. V. Ramanathan *et al.*, *Science* **243**, 57 (1989); E. F. Harrison *et al.*, *J. Geophys. Res.* **95**, 18687 (1990).
2. R. J. Charlson, *et al.*, *Nature* **326**, 655 (1987).
3. E. M. Feigelson, *Beitr. Phys. Atmos.* **51**, 203 (1978); A. K. Bates and Harshvardhan, *J. Geophys. Res.* **92**, 8483 (1987).
4. G. P. Ayers, *et al.*, *Nature* **349**, 404 (1991).
5. T. S. Bates, B. K. Lamb, A. Geunther, J. Dignon, R. E. Stoiber, *J. Atmos. Chem.*, in press.
6. We distinguished low-level clouds from high-level clouds using the filter $[F(\text{clear}) - F(\text{overcast})]/F(\text{clear}) < 0.125$, where F(clear) is the monthly mean clear-sky longwave flux at a scanning point and F(overcast) is the instantaneous overcast longwave flux at a scanning point (F values are in watts per square meter). Sea ice cover was determined on the basis of climatological data.
7. H. R. Gordon, J. W. Brown, R. H. Evans, *Appl. Opt.* **27**, 862 (1988); C. R. McClain, G. C. Feldman, W. E. Esaias, in *Global Change Atlas*, C. Parkinson, J. Foster, R. Gurney, Eds. (Cambridge Univ. Press, Cambridge, in press).
8. Spatial autocorrelation analysis revealed that albedo was autocorrelated with a length scale of 3° of longitude whereas chlorophyll was autocorrelated with a length scale of 5° of longitude. We spatially averaged the albedo data to conform to the chlorophyll length scale. For further comparison, chlorophyll data were shifted 400 km downwind (to the east), conforming to the optimal cross-correlation between the two variables.
9. "The 1985 NAPAP (National Acid Precipitation Assessment Program) emissions inventory (Version 2): Development of the annual data on modeler's tapes" (Publ. EPA-600/7-89-012a, Environmental Protection Agency, Washington, DC, 1989).
10. Y.-J. Han and S.-W. Lee, *Mon. Weather Rev.* **111**, 1554 (1983).
11. C. Leck, *et al.*, *J. Geophys. Res.* **95**, 3353 (1990); T. S. Bates, *et al.*, *Nature* **329**, 319 (1987); P. M. Holligan, *et al.*, *Cont. Shelf. Res.* **7**, 273 (1987).
12. M. D. Keller, W. K. Bellow, R. R. L. Guillard, in *Biogenic Sulfur in the Environment*, E. S. Saltzman and W. J. Cooper, Eds. (American Chemical Society, Washington, DC, 1989), pp. 167–182; M. O. Andreae, W. R. Barnard, J. M. Ammons, *Ecol. Bull. (Stockholm)* **35**, 167 (1983).
13. P. M. Holligan and W. M. Balch, in *Particle Analysis in Oceanography*, S. Demers, Ed. (Springer-Verlag, New York, 1991), pp. 301–324.
14. D. L. Savole and J. M. Prospero, *Nature* **339**, 685 (1989); A. M. Thompson, W. E. Esaias, R. L. Iverson, *J. Geophys. Res.* **95**, 20551 (1990).
15. Product moment correlation analysis indicated that, of the 22 analyzable cases, albedo and chlorophyll were significantly ($P \leq 0.10$) positively correlated in 11 and significantly negatively correlated in 1. Albedo and SST were significantly positively correlated in 9 and significantly negatively correlated in 5. A two-parameter linear model using SST and chlorophyll accounted for more than 50% of the variance in albedo in 14 cases.
16. R. J. Charlson *et al.*, *Science* **255**, 423 (1992).
17. R. J. Charlson, J. Langer, H. Rodhe, C. B. Levoy, S. G. Warren, *Tellus Ser. AB* **43**, 152 (1991).

18. This research was supported by the U.S. Department of Energy, the National Aeronautics and Space Administration, and the Electric Power Research Institute. We thank S. Schwartz, P. Minnett, P. Michael, A. Morel, P. Holligan, and R. Charlson for discussions, and G. Feldman for providing the global CZCS data set.

11 December 1991; accepted 23 March 1992

Functional Specialization of Olfactory Glomeruli in a Moth

Bill S. Hansson,* Håkan Ljungberg, Eric Hallberg, Christer Löfstedt

The specific function of the glomerular structures present in the antennal lobes or olfactory bulbs of organisms ranging from insects to humans has been obscure because of limitations in neuronal marking methods. By tracing individual neurons in the moth *Agrotis segetum*, it was determined that physiologically distinct types of pheromone receptor neurons project axons to different regions of the macroglomerular complex (MGC). Each glomerulus making up the MGC has a specific functional identity, initially processing information about one specific pheromone component. This indicates that, at least through the first stage of synapses, olfactory information moves through labeled lines.

Olfactory glomerulus function has been studied by a variety of methods, including activity mapping by deoxyglucose injections (*1*, *2*) or tracing by antero- or retrograde filling of afferent neurons (*3–6*). These studies have involved large numbers of sensory cells and have thus shown activation of large areas in the olfactory bulbs or lobes, or filling of large numbers of neurons of unknown specificity. We have here recorded electrophysiologically from single, pheromone-specific receptor cells on

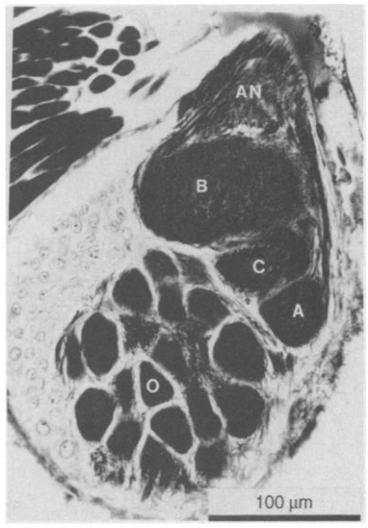

Fig. 1. Section through the antennal lobe in a male *Agrotis segetum*. The enlarged macroglomerular complex is situated close to the entrance of the antennal nerve (AN) and contains four glomerular units (A, B, C, and D). In this section subunit D is not visible. Below the MGC a cluster of ordinary glomeruli (O) is situated.

Table 1. Summary of sensillum fills (*20*). Numbers in parentheses indicate how many cells were filled with each stimulus. Numbers below glomeruli A, B, C, and D indicate how many neurons projected to each glomerulus from the different sensillum types, when stimulated with the respective stimuli.

Stimulus	Z5-10:OAc			Z7-12:OAc		Z9-14:OAc	
	A	B	A+B	C	C+B	D	D+B
Z5-10:OAc (18)	5	1	12	0	0	0	0
Z5-10:OH (11)	1	7	3	0	0	0	0
Z7-12:OAc (10)	0	0	0	6	4	0	0
Z9-14:OAc (1)	0	0	0	0	0	0	1

a male moth antenna, and subsequently defined these cells morphologically, to study the projections of individual, afferent olfactory neurons. The results show functional separation of the glomerular subdivisions present in the male moth MGC, which is known to be responsible for the initial integration of information about sex pheromones in the male moth brain (*7–10*). Three different types of sensory cells, each activated by a different pheromone component, project to three morphologically defined subunits of the MGC.

Pheromone-sensitive olfactory sensilla on the male turnip moth *Agrotis segetum* (Lepidoptera; Noctuidae) antenna were

B. S. Hansson and C. Löfstedt, Department of Ecology, Lund University, S-223 62 Lund, Sweden.
H. Ljungberg and E. Hallberg, Department of Zoology, Lund University, S-223 62 Lund, Sweden.
*To whom correspondence should be addressed.

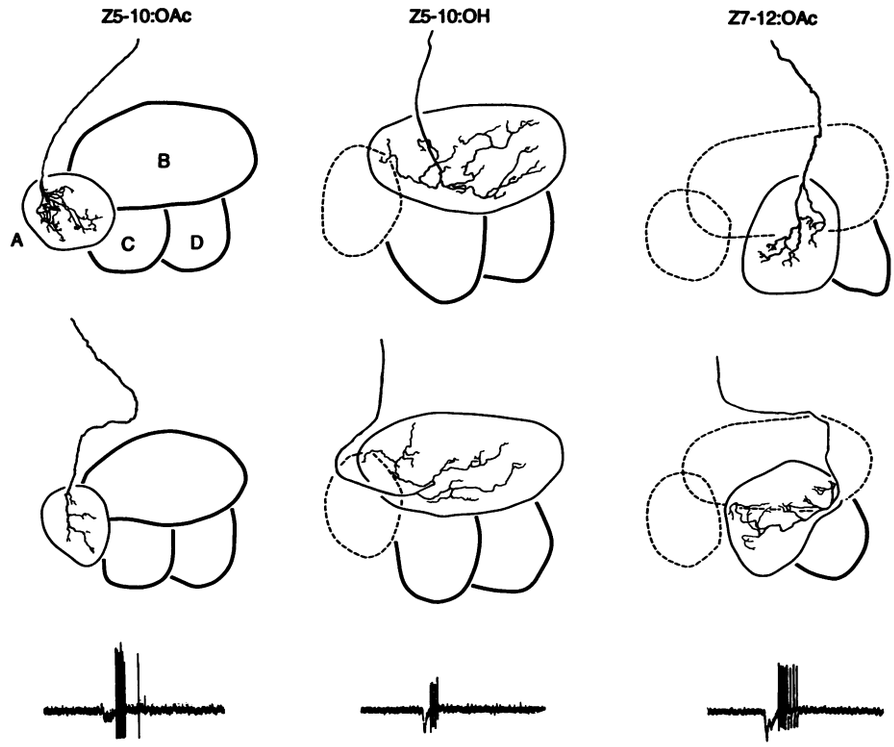

Fig. 2. Typical examples of serial reconstructions of single olfactory afferents filled in the experiments. The different physiological types are indicated by their pheromone component specificity. Two examples of each type are presented. The outline of the glomerular unit innervated is indicated by a thin line, the units situated behind it in a frontal section are indicated by a thicker line, and the ones situated in front by a dotted line. The letter designations of the four glomerular units (A, B, C, and D) according to Fig. 1 are shown in one reconstruction, for comparison. Note that Fig. 1 shows an MGC from the right antennal lobe of the moth brain, whereas the reconstructions show left lobe MGCs. Below each reconstruction the physiological response of that receptor neuron to its key stimulus is represented. The response of a cell to stimulation by the two components for which it was not specific was zero.

classified by electrophysiological response of one of the two cells present in a sensillum to pheromone components. Three types of sensilla occur, each containing a cell specifically tuned to one of the three pheromone components: (Z)-5-decenyl acetate (Z5-10:OAc), (Z)-7-dodecenyl acetate (Z7-12:OAc), or (Z)-9-tetradecenyl acetate (Z9-14:OAc). Of 3000 sensilla tested, 66% responded to Z5-10:OAc, 33% to Z7-12:OAc, and much less than 1% responded to Z9-14:OAc. Each of the sensillum types contains an additional cell. In sensilla responsive to Z5-10:OAc, the second cell is stimulated by Z5-10:OH. The key stimulus for the second cell in the other two sensillum types is not known.

Olfactory cells of physiologically identified sensilla were filled anterogradely with cobalt lysine (*12*). The insect brain was subsequently dissected, and filled cells were visualized by silver intensification of the cobalt. Axonal projections of the olfactory receptor cells in the antennal lobes were reconstructed from 10-μm sections. Attempted fillings of cells in ten sensilla without odor stimulation all failed, whereas nine out of ten attempts of filling during stimulation were successful ($P < 0.001$, Fisher's exact probability test).

Four general subdivisions are apparent in the MGC (Fig. 1) (*13*). When the neurons from the three types of sensilla were reconstructed, different projection patterns emerged (Fig. 2). Cells in the Z5-10:OAc sensillum type always projected into regions A and B, cells in the Z7-12:OAc sensillum projected into regions B and C, and cells in the Z9-14:OAc sensillum projected into regions B and D. In 20 out of 40 successful fills, only one of the two cells contained in a sensillum filled. Challenging the Z5-10:OAc sensillum with Z5-10:OAc resulted mainly in fills projecting to the A region, whereas stimulation with Z5-10:OH resulted in a dominance of projections to the B region. The selective filling of regions A and B from the two cells housed in the Z5-10:OAc sensillum was statistically significant ($P = 0.016$, Fisher's exact probability test) (Table 1). Six single fills of the Z7-12:OAc sensillum, stimulated with Z7-12:OAc, all projected to region C. Our interpretation of the data is thus that the

Z5-10:OAc–specific cell type projects to MGC subunit A situated in the medial part of the MGC. In this sensillum type the second cell, responsive to Z5-10:OH, terminates in MGC subunit B, close to the entrance of the antennal nerve into the antennal lobe. The cell responsive to Z7-12:OAc projects to MGC subunit C, situated in the middle of the MGC. In the same sensillum, a second cell of unknown specificity projects to subunit B. In approximately 3000 contacts made with olfactory sensilla during this investigation only one Z9-14:OAc–specific cell was encountered. In this sensillum two cells were filled. One terminates in subunit D, ventral and posterior to the other subunits. As in the other two physiological sensillum types, the second cell projects to subunit B. No correlation was observed between the topographical situation of sensilla on the antenna and their projection into the MGC subunits.

Filling of the second, unstimulated neuron in a sensillum may depend on neural activity induced after prolonged stimulation of the other cell in the sensillum. For example, in the Z5-10:OAc sensillum, buildup of the hydrolysis product of Z5-10:OAc, namely Z5-10:OH, may serve as the stimulus for the nonstimulated cell.

Selective filling of neurons present in the same sensillum has been used to investigate central nervous projections of taste receptors present on the labellum of *Drosophila*. By using horseradish peroxidase cocktails laced with the stimulus for one of the receptor cells present in the sensillum, different cell types were filled (*14*). The response characteristics of the sensilla investigated were, however, not known.

Functional partitioning in the primary olfactory center has been analyzed in rats (*3–5*), crayfish (*15*), cockroaches (*16, 17*), fruit flies (*2, 6*), and moths (*18, 19*). In *Drosophila*, studies with 2-deoxyglucose have until now presented the strongest evidence for a functional partitioning of the antennal lobe (*2, 6*). In the moths *Manduca sexta* (*17*) and *Heliothis virescens* (*18*), single projection neurons of known specificity were identified morphologically, and the dendritic trees of some of these were clearly confined to different glomerular parts of the MGC. However, other types of projection neurons did not confirm the pattern (*17, 18*). Projection of single neurons was also analyzed in the cockroach *Periplaneta*, but no clear structure-function relation was observed (*15, 16*). These studies have indicated that there might be functional significance to the arrangements of glomerular structures in the olfactory pathway.

We show here that specific identifiable olfactory receptor types project to distinctly separated glomerular structures in the MGC of the antennal lobe, thus strongly indicating that these are functionally distinct units.

REFERENCES AND NOTES

1. G. Arnold and C. Masson, *C. R. Acad. Sci.* **305**, 271 (1987).
2. V. Rodriguez, *Brain Res.* **453**, 299 (1988).
3. L. Astic, D. Saucier, A. Holley, *ibid.* **424**, 144 (1987).
4. P. J. Jastreboff *et al.*, *Proc. Natl. Acad. Sci. U.S.A.* **81**, 5250 (1984).
5. P. E. Pedersen, P. J. Jastreboff, W. B. Stewart, G. M. Shepherd, *J. Comp. Neurol.* **250**, 93 (1986).
6. R. F. Stocker, R. N. Singh, M. Schorderet, O. Siddiqi, *Cell Tissue Res.* **232**, 237 (1983).
7. J. Boeckh and V. Boeckh, *J. Comp. Physiol. A* **132**, 235 (1979).
8. S. G. Matsumoto and J. G. Hildebrand, *Proc. R. Soc. London Ser. B* **213**, 249 (1981).
9. T. A. Christensen and J. G. Hildebrand, in *Arthropod Brain: Its Evolution, Development, Structure, and Functions*, A. P. Gupta, Ed. (Wiley, New York, 1987), pp. 457–483.
10. A. M. Schneiderman, S. G. Matsumoto, J. G. Hildebrand, *Nature* **298**, 844 (1982).
11. C. Löfstedt *et al.*, *J. Chem. Ecol.* **8**, 1305 (1982).
12. The receptor neurons were typed physiologically by the tip recording method [K.-E. Kaissling, in *Biochemistry of Sensory Functions*, L. Jaenicke, Ed. (Springer-Verlag, Berlin, 1974), pp. 243–273; J. N. C. Van Der Pers and C. J. Den Otter, *J. Insect. Physiol.* **24**, 337 (1978)] with 0.5 M cobalt lysine as the electrode electrolyte. When contact had been established, the sensillum was typed by stimulation by the three stimuli known to stimulate one receptor neuron in each of the three physiological sensillum types present on the male *Agrotis segetum* antenna. The stimulus was then pulsed onto the antenna. The pulses were typically 50 ms, at 0.5 Hz, with an air flow of 1 ml/s. The preparation was stimulated for 1 hour. The receptor neuron typically continued to spike during the whole filling period. The insect was placed at 8°C for 48 hours and then dissected. The brain of the insect was treated according to standard methods for silver intensification of cobalt fills [M. Obermayer and N. J. Strausfeld, in *Neuroanatomical Techniques, Insect Nervous System*, N. J. Strausfeld and T. A. Miller, Eds. (Springer-Verlag, Berlin, 1980), pp. 406–430], after which the preparation was cleared with methyl salicylate. The neurons were observed and photographed in the whole preparation, and brains containing fills were then embedded in epoxy resin (Durcupan, Fluka). The brain was cut into 10-μm-thick sections, which were counterstained with methylene blue. The sections were photographed in three to five different focal depths each, and the slides produced were used to perform the serial reconstruction of each neuron. This procedure made it possible to establish unambiguously in which subglomerular unit the axonal branches were situated.
13. The brains used for reconstructions were fixed in alcoholic Bouin's solution and then were treated according to Rowell's silver staining method [C. H. F. Rowell, *Q. J. Microsc. Sci.* **104**, 81 (1963)]. After embedding in paraffin, the preparations were sectioned in 10-μm sections and were studied under a light microscope. Photographs of the sections were then used as a basis for serial reconstruction of the MGC.
14. S. R. Shanbhag and R. N. Singh, *Cell Tissue Res.* **267**, 273 (1992).
15. D. Mellon, Jr., and S. D. Munger, *J. Comp. Neurol.* **296**, 253 (1990).
16. M. Burrows, J. Boeckh, J. Esslen, *J. Comp. Physiol. A* **15**, 447 (1982).
17. M. Hösl, *ibid.* **167**, 321 (1990).
18. B. S. Hansson, T. A. Christensen, J. G. Hildebrand, *J. Comp. Neurol.* **312**, 264 (1991).
19. T. A. Christensen, H. Mustaparta, J. G. Hildebrand, *J. Comp. Physiol. A* **169**, 259 (1991).
20. Either one or two cells were filled in each sensillum. The cell specific for the stimulus applied filled exclusively in about half of the fills. We tested the selectiveness of the filling method by comparing the filling frequencies of the two cells present in the Z5-10:OAc sensillum by Fisher's exact test [R. R. Sokal and F. J. Rohlf, *Biometry* (Freeman, San Francisco, 1981)], which gave a P value of 0.016. The selectiveness was thus statistically significant.

21. We thank M. Johansson and E. Sjögren for rearing the insects, and R. Cantera and R. Finlay for comments on the manuscript.

15 January 1992; accepted 10 April 1992

Association of a 59-Kilodalton Immunophilin with the Glucocorticoid Receptor Complex

Ping-Kaung Ku Tai, Mark W. Albers, Hong Chang, Lee E. Faber, Stuart L. Schreiber*

Immunophilins, a family of proteins that exhibit rotamase (peptidyl-prolyl *cis-trans* isomerase) activity in vitro, are expressed in many organisms and most tissues. Although some immunophilins can mediate the immunosuppressive actions of FK506, rapamycin, and cyclosporin A, the physiological role of the unligated proteins is not known. A 59-kilodalton member of the FK506- and rapamycin-binding class was found to associate in the absence of these drugs with two heat shock proteins (hsp90 and hsp70) and the glucocorticoid receptor (GR). Together, these proteins make up the inactive GR, thus biochemically linking two families of proteins proposed to be involved in protein folding and assembly as well as two potent immunosuppressive modalities.

Immunophilins are proteins that bind the immunosuppressants FK506, rapamycin, and cyclosporin A (CsA) (*1*). Immunophilins are comprised of two classes: the FK506- and rapamycin-binding proteins (FKBPs) and the CsA-binding cyclophilins. Certain members of each class mediate the ability of the drugs to block intermediate steps along specific signal transduction pathways in a variety of cell types (*2, 3*). Although all known immunophilins have rotamase (peptidyl-prolyl *cis-trans* isomerase) activity in vitro, the relevance of this activity in vivo is unknown. Thus, the cellular role of these